Available online at www.sciencedirect.com
ScienceDirect
Journal of Computational and Applied Mathematics 203 (2007) 419–436
JOURNAL OF COMPUTATIONAL AND APPLIED MATHEMATICS
www.elsevier.com/locate/cam

An ODE traffic network model

M. Herty, A. Klar, A.K. Singh*, [1]

Technomathematics Group, University of Technology Kaiserslautern, P.O. Box 3049, D-67653 Kaiserslautern, Germany

Received 29 November 2004; received in revised form 7 July 2005

Abstract

We are interested in models for vehicular traffic flow based on partial differential equations and their extensions to networks of roads. In this paper, we simplify a fluidodynamic traffic model and derive a new traffic flow model based on ordinary differential equations (ODEs). This is obtained by spatial discretization of an averaged density evolution and a suitable approximation of the coupling conditions at junctions of the network. We show that the new model inherits similar features of the full model, e.g., traffic jam propagation. We consider optimal control problems controlled by the ODE model and derive the optimality system. We present numerical results on the simulation and optimization of traffic flow in sample networks.

MSC: 90B10; 90B20; 49J15

Keywords: Network models; Adjoint calculus; Traffic flow

1. Introduction

Nowadays, there exists a broad range of traffic flow models describing different features and properties of vehicular traffic flow. The class of so-called macroscopic models describe traffic in terms of averaged quantities like density or flow. There are other models dealing with individual cars [11,12] or probability functions [16,18]. Macroscopic traffic flow modelling started with the work of Ligthill and Whitham [23] in the 1950th. They introduced a scalar conservation law to describe the evolution of the car-density. Later extensions are proposed which have been subject of intense discussions [1,10,25]. First, extensions to traffic flow on road networks arise in [8,13–15]. Our starting point is the model introduced in [8]. We derive an approximation to this model by a three-point spatial discretization and suitable coupling conditions. The final model consists of a system of coupled ordinary differential equations (ODEs model). We qualitatively compare the simplified model and the original model based on partial differential equations by considering different traffic situations and by comparing computing times. Finally, we introduce an optimal control problem for the ODE model. We derive the first-order optimality system with adjoint and gradient equations. We optimize the traffic distribution in some sample networks using different optimization methods.

* Corresponding author.
E-mail addresses: herty@mathematik.uni-kl.de (M. Herty), klar@mathematik.uni-kl.de (A. Klar), singh@mathematik.uni-kl.de (A.K. Singh).
[1] Supported by German Research Foundation-Graduiertenkolleg 853/1-03, University of Technology Darmstadt.

0377-0427/$ - see front matter © 2006 Elsevier B.V. All rights reserved.
doi:10.1016/j.cam.2006.04.007

In Section 2, we describe the underlying PDE traffic network model and the simplifications. Further the coupling conditions at certain type of junctions are discussed. The new traffic flow model is introduced in Section 2.5. Section 3 introduces the optimal control problem and the optimality system. We present numerical examples in Section 4.

2. Traffic network models

2.1. Macroscopic PDE model

The macroscopic models describe average properties of vehicular traffic flow. Following [23], the function $\rho(x,t)$ describes the car-density at a point x and a time t. The evolution of ρ is given by a scalar conservation law resembling the conservation of cars. Before we discuss more modelling details, we introduce a network of roads: a network of roads is modelled [8,13] as a finite, directed and connected graph. Each edge models a single road and each vertex a junction. We further model each road $j=1,\dots,I$ by an interval $[a_j,b_j]$, where a_j or b_j can be infinity if and only if the road is incoming to or outgoing from, respectively, the network.

We model the density on each road j by a function $\rho_j(x,t)$. Further, we denote by $\rho_{\max,j}$ the maximal density on road j corresponding to the situation where cars stand bumper to bumper. We assume [23,24] a relation (the so-called "fundamental diagram") between the density ρ_j and the flux $f_j=\rho_j v_j$, where v_j is the average velocity of cars on road j. There has been intense discussion on the justification of the "fundamental diagram", but measurements on highways suggest, that there exists a connection [19,21] and that this can be modelled by a concave function $f(\rho)$ with a single maximum. Therefore, we assume that there exists a family of flux-functions f_j such that for each $j=1,\dots,I$

$$f_j \text{ is continuously differentiable on } [0,\rho_{\max,j}], \tag{1}$$

$$f_j(0)=f_j(\rho_{\max,j})=0, \tag{2}$$

$$f_j \text{ is strictly concave}, \tag{3}$$

$$\exists \sigma_j\in(0,\rho_{\max,j}) : f_j'(\sigma_j)=0. \tag{4}$$

For example, let $f_j(\rho)=4\rho(1-\rho/\rho_{\max})$. Then, the macroscopic Lighthill–Whitham model for traffic flow on a road j is given by the non-linear conservation law

$$\frac{\partial\rho_j(x,t)}{\partial t}+\frac{\partial f_j(\rho_j(x,t))}{\partial x}=0 \quad \forall x\in[a_j,b_j],\ t\in[0,T], \tag{5}$$

$$\rho_j(x,0)=\rho_{j,0}(x) \quad \forall x\in[a_j,b_j]. \tag{6}$$

It remains to discuss the coupling conditions at junctions stated in [8]. We consider a single junction with n roads labelled by $j=1,\dots,n$ with end b_j at the junction and m roads labelled by $j=n+1,\dots,n+m$ with end a_j at the junction. To guarantee the conservation of the numbers of cars, at the junction the following condition is prescribed:

$$\sum_{j=1}^{n} f_j(\rho_j(b_j,t))=\sum_{j=n+1}^{n+m} f_j(\rho_j(a_j,t)) \quad \forall t\geqslant 0. \tag{7}$$

However, this condition does not suffice to determine a unique solution on the network in the sense made precise below. Therefore, authors introduce a matrix $A\in R^{m\times n}$, where $(A)_{ji}=a_{ji}$ ($j\in\{n+1,\dots,n+m\}, i\in\{1,\dots,n\}$) describes the percentage of drivers who want to drive (and also must drive) from road i to road j in [8]. The matrix A is assumed to fulfill the following assumptions:

$$a_{ji}\neq a_{ji'}\ \forall i\neq i' \quad \text{and} \quad 0<a_{ji}<1 \quad \text{and} \quad \sum_{j=n+1}^{n+m} a_{ji}=1\ \forall i\in\{1,\dots,n\}. \tag{8}$$

We refer to Section 3 for a motivation and interpretation of the matrix A.

We state the boundary conditions at a junction for weak solutions. A weak solution at a junction is a collection of functions $\rho_j : [0,\infty)\times[a_j,b_j]\to\mathbb{R}$ for $i=1,\dots,n+m$ s.t.

$$\sum_{i=1}^{n+m}\int_0^\infty\int_{a_j}^{b_j}\left(\rho_i\partial_t\phi_i + f(\phi_i)\partial_x\phi_i\right)\,\mathrm{d}x\,\mathrm{d}t = 0, \tag{9}$$

for each ϕ_i, $i=1,\dots,n+m$, is a smooth function and having compact support in $\mathbb{R}\times(0,\infty)$ and is smooth across the junction, i.e., for $i=1,\dots,n$, $j=n+1,\dots,n+m$

$$\phi_i(b_i,\cdot)=\phi_j(a_j,\cdot),\quad \partial_x\phi_i(b_i,\cdot)=\partial_x\phi_j(a_j,\cdot).$$

Note that (9) implies (7) if the functions ρ_i are sufficiently regular. If $\rho_j(t,\cdot)$ are functions of bounded variation we additionally assume that the following properties are satisfied:

$$f(\rho_j(a_j+,\cdot)) = \sum_{i=1}^{n}\alpha_{ji}\,f(\rho_i(b_i-,\cdot)),\quad j=n+1,\dots,n+m, \tag{10}$$

$$\sum_{i=1}^{n} f(\rho_i(b_i-,\cdot)) + \sum_{i=n+1}^{n+m} f(\rho_i(a_i+,\cdot)) \text{ is maximal w.r.t. (10).} \tag{11}$$

The following result concerning existence and uniqueness is known.

Theorem 1 (*Coclite et al. [8, Theorem 8.2]*). *Consider a flux function f_j satisfying* (5) *and a road network in which all the junctions have at most two ingoing and two outgoing roads. Let $\bar\rho=(\rho_1,\dots,\rho_I)$ be an initial data in L^1_{loc} and $T>0$ fixed. Then there exists an unique admissible solution $\rho=(\rho_1,\dots,\rho_I)$, $\rho_j:[a_j,b_j]\times[0,T]\to\mathbb{R}$ with $\rho(\cdot,0)=\bar\rho$.*

A main step in the proof of existence and uniqueness of admissible weak solutions is the consideration of constant initial data $\rho_{j,0}$ and for one junction only. An admissible solution can be constructed as follows. We introduce for each road j an intermediate state $\overline{\rho}_j\in\mathbb{R}$, $j=1,\dots,n+m$. The solution $\rho_j(x,t)$ to the problem (5) and (7) is given as solution to a Riemann problem on each road j. For incoming roads the initial conditions for the Riemann problem are

$$\rho_j(x,0)=\begin{cases}\rho_{j,0}, & x\leqslant b_j,\\ \overline{\rho}_j^b, & x>b_j\end{cases} \tag{12}$$

and similar for outgoing roads with the state $\overline{\rho}_j^a$. Hereby, we impose certain restrictions to the values $\overline{\rho}_j^{a,b}$. We assume $\overline{\rho}_j^a,\overline{\rho}_j^b$ to be independent of time, that is all waves of the Riemann problems have to emerge from the junction, i.e., have non-positive speed for ingoing and non-negative for outgoing roads.

Note that the existence theorem only covers junctions with a total of four connected roads. Further, the construction of the states $\overline{\rho}_j^{a,b}$ is not explicit in a case with more than three connected roads. Therefore, we restrict our discussion to the cases of three connected roads and give the precise formulas for the intermediate states $\overline{\rho}_j^{a,b}$ and we can rephrase the traffic model as coupled system of partial differential equations with explicit boundary values. Further, by composition of such junctions we can easily model all other kinds of possible junctions.

There are two possibilities of junctions with a total of three connected roads: either one road disperses into two roads or two roads merging into one road.

2.2. Dispersing junction

The incoming road is labelled as j_1 and two outgoing roads are labelled as j_2, j_3, respectively. According to [8] the matrix A is $A=[\alpha,1-\alpha]$, where $0\leqslant\alpha\leqslant1$. By assumption, the strictly concave flux functions f_j have a unique,

single maximum denoted by σ_j and therefore f_j are invertible on $[0, \sigma_j]$ and $[\sigma_j, 1]$, and denote the inverse by $f_j^{-1,+}$ and $f_j^{-1,-}$, respectively.

Assume $\rho_{j,0}$ is constant and let the constants c_j be

$$c_{j_1} = \begin{cases} f_{j_1}(\rho^{(b)}_{j_1,0}), & \rho^{(b)}_{j_1,0} < \sigma_{j_1}, \\ f_{j_1}(\sigma_{j_1}), & \rho^{(b)}_{j_1,0} > \sigma_{j_1}, \end{cases} \tag{13}$$

$$c_k = \begin{cases} f_k(\rho^{(a)}_{k,0}), & \rho^{(a)}_{k,0} > \sigma_k, \\ f_k(\sigma_k), & \rho^{(a)}_{k,0} < \sigma_k, \end{cases} \qquad k = j_2, j_3, \tag{14}$$

$$\gamma = \min\left\{ c_{j_1}, \frac{c_{j_2}}{\alpha}, \frac{c_{j_3}}{1-\alpha} \right\}. \tag{15}$$

Then we obtain the following closed formulas for $\overline{\rho}_j^{a,b}$:

$$\overline{\rho}^b_{j_1} = \begin{cases} \rho^{(b)}_{j_1,0}, & \rho^{(b)}_{j_1,0} < \sigma_{j_1}, \gamma = c_{j_1}, \\ f_{j_1}^{-1,+}(\gamma) & \text{else}, \end{cases} \tag{16}$$

$$\overline{\rho}^a_{j_2} = \begin{cases} \rho^{(a)}_{j_2,0}, & \rho^{(a)}_{j_2,0} > \sigma_{j_2}, \gamma = c_{j_2}/\alpha, \\ f_{j_2}^{-1,-}(\alpha\gamma) & \text{else}, \end{cases} \tag{17}$$

$$\overline{\rho}^a_{j_3} = \begin{cases} \rho^{(a)}_{j_3,0}, & \rho^{(a)}_{j_3,0} > \sigma_{j_3}, \gamma = c_{j_3}/(1-\alpha), \\ f_{j_3}^{-1,-}((1-\alpha)\gamma) & \text{else}. \end{cases} \tag{18}$$

As discussed in more detail in [8,13], the above conditions guarantee by construction that, (7) is satisfied, all waves have the "correct" wave speeds and the flux on the incoming roads is maximal subject to the conditions.

2.3. Merging junction

Let incoming roads to the junction are labelled as j_1, j_2 and the outgoing road as j_3. The initial densities on roads j are given by $\rho_{j,0}$ for $j \in \{j_1, j_2, j_3\}$ and are assumed to be constant.

Let $\gamma_{j,0} = f(\rho_{j,0})$ and let c_j be

$$c_k = \begin{cases} f_k(\rho^{(b)}_{k,0}), & \rho^{(b)}_{k,0} < \sigma_k, \\ f_k(\sigma_k), & \rho^{(b)}_{k,0} > \sigma_k, \end{cases} \qquad k = j_1, j_2, \tag{19}$$

$$c_{j_3} = \begin{cases} f_{j_3}(\rho^{(a)}_{j_3,0}), & \rho^{(a)}_{j_3,0} > \sigma_{j_3}, \\ f_{j_3}(\sigma_{j_3}), & \rho^{(a)}_{j_3,0} < \sigma_{j_3}. \end{cases} \tag{20}$$

Combining results of [13,8], we continue and distinguish, if $c_{j_1} + c_{j_2} \leqslant c_{j_3}$, then

$$\gamma_{j_1} = c_{j_1}, \quad \gamma_{j_2} = c_{j_2} \quad \text{and} \quad \gamma_{j_3} = \gamma_{j_1} + \gamma_{j_2} \tag{21}$$

else if $c_{j_1} + c_{j_2} > c_{j_3}$, then

$$\gamma_{j_1} = \gamma_{j_2} = \min\{c_{j_1}, c_{j_2}, c_{j_3}/2\}, \tag{22}$$

$$\gamma_{j_3} = \gamma_{j_1} + \gamma_{j_2}. \tag{23}$$

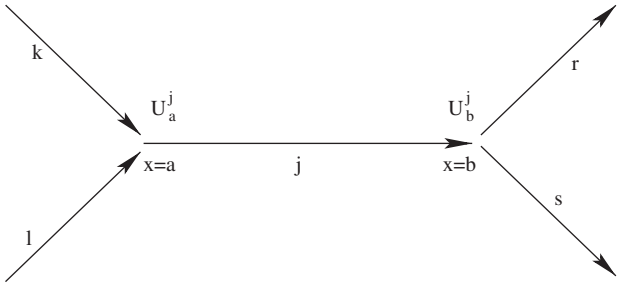

Fig. 1. Coupling condition at the junction.

Note that the coupling in the second case (23) resembles a first-in–first-out principle. In that particular situation the inflow $\gamma_{j_1} + \gamma_{j_2}$ is larger than the maximal possible outflow. Therefore, we require that cars enter in an alternating way into the outgoing road j_3. This explains the factor $\frac{1}{2}$ appearing in the calculation of the actual flow at the junction.

Finally, we can define the states $\overline{\rho}_j^{a,b}$

$$\overline{\rho}_k^b = \begin{cases} \rho_k^{(b)}, & \rho_k^{(b)} < \sigma_k, \gamma_k = c_k, \\ f_k^{-1,+}(\gamma_k) & \text{else}, \end{cases} \qquad k = j_1, j_2, \tag{24}$$

$$\overline{\rho}_{j_3}^a = \begin{cases} \rho_{j_3}^{(a)}, & \rho_{j_3}^{(a)} > \sigma_{j_3}, \gamma_{j_3} = c_{j_3}/2, \\ f_{j_3}^{-1,-}(\gamma_3) & \text{else}. \end{cases} \tag{25}$$

2.4. Summary of the coupling conditions

By the above discussion, we determine $\overline{\rho}_j^{a,b}$ uniquely and we obtain a solution $\rho_j(x,t)$ for constant initial data by solving the Riemann problems. The solution to a problem with non-constant initial data is obtained by wave or front-tracking [5].

We introduce the following notation. Fix a road j and consider the situation depicted in Fig. 1, i.e., at $x = a_j$ a junction connects roads j, k, l and at $x = b_j$ another junction connects the roads j, r, s. For given values ρ_j, ρ_r, ρ_s and ρ_j, ρ_k, ρ_l we define the functions U_a^j and U_b^j, respectively, by

$$U_b^j(\rho_j, \rho_r, \rho_s, \alpha) := \overline{\rho}_j^b, \quad U_a^j(\rho_j, \rho_k, \rho_l) := \overline{\rho}_j^a,$$

where $0 \leqslant \alpha \leqslant 1$ is fixed and where $\overline{\rho}_j^a$ and $\overline{\rho}_j^b$ are given by the discussion in Sections 2.2 and 2.3, respectively.

Finally, the PDE model for on a single road j connected on both sides to junctions as in Fig. 1 reads

$$\frac{\partial \rho_j(x,t)}{\partial t} + \frac{\partial f_j(\rho_j(x,t))}{\partial x} = 0 \quad \forall x \in [a_j, b_j], t > 0, \tag{26}$$

$$\rho_j(x,0) = \rho_{j,0}(x) \quad \forall x \in [a_j, b_j], \tag{27}$$

$$\rho_j(a,t) = U_a^j(\rho_j(a,t-), \rho_k(b,t-), \rho_l(b,t-)) \quad \forall t > 0, \tag{28}$$

$$\rho_j(b,t) = U_b^j(\rho_j(b,t-), \rho_r(a,t-), \rho_s(a,t-), \alpha) \quad \forall t > 0. \tag{29}$$

Remark 2. According to [8], Theorem 1 holds true in the case $A = A(t)$, i.e., time-dependent distributions of the flux at junctions. The simplified models below also remain valid even in this case. For simplicity, we deal only with the case of time-independent controls.

Furthermore, the coupling conditions allow shock waves (corresponding to traffic jams) to pass a junction. This implies that a crowed outgoing road may generate a traffic jam on any incoming road.

2.5. Macroscopic ODE models

Of course, the solution of a PDE traffic network model is time consuming and cannot be done in real-time even with appropriate schemes. We report later on computation times which support this fact. The situation is more severe in case of the optimal control problems governed by the PDE model, since each optimization step usually requires several simulations of the governing equations. Therefore, we present a simplified model obtained by spatial discretization of the PDE. To be more precise, based on averaged density evolution of traffic on each road, we perform simple finite spatial discretization of (5) and obtain ODE models. For notational simplicity, we drop the subscripts for a_j, b_j and $L_j = b_j - a_j$ in the following.

After integrating (5) over $[a, d]$ and $[d, b]$, $a < d = (a + b)/2 < b$ we obtain

$$\partial_t \rho_j^{(a)}(t) = -\frac{2}{L}(f(\rho_j(d, t)) - f(\rho_j(a, t))), \tag{30}$$

$$\partial_t \rho_j^{(b)}(t) = \frac{2}{L}(f(\rho_j(d, t)) - f(\rho_j(b, t))), \tag{31}$$

where $L = b - a$ is the length of the road and where the spatial approximations are

$$\rho_j^{(a)}(t) = \frac{2}{L}\int_a^d \rho_j(x, t)\,\mathrm{d}x \quad \text{and} \quad \rho_j^{(b)}(t) = \frac{2}{L}\int_d^b \rho_j(x, t)\,\mathrm{d}x.$$

Eqs. (30), (31) contain additional unknowns. For $\rho_j(d, t)$ we assume, that the half-sum is a reasonable approximation and set:

$$\rho_j(d, t) = \tfrac{1}{2}(\rho_j^{(a)}(t) + \rho_j^{(b)}(t)). \tag{32}$$

Initial conditions are obtained by averaging

$$\rho_{j,0}^{(a)} = \frac{2}{L}\int_a^d \rho_{j,0}(x)\,\mathrm{d}x \quad \text{and} \quad \rho_{j,0}^{(b)} = \frac{2}{L}\int_d^b \rho_{j,0}(x)\,\mathrm{d}x. \tag{33}$$

Finally, we obtain the values $\rho_j(a, t)$ and $\rho_j(b, t)$ by the coupling conditions of the previous sections, i.e., we define

$$\overline{\rho}_j^a(t) = U_a^j(\rho_j^{(a)}(t), \rho_k^{(a/b)}(t), \rho_l^{(a/b)}(t)), \tag{34}$$

$$\overline{\rho}_j^b(t) = U_b^j(\rho_j^{(b)}(t), \rho_r^{(a/b)}(t), \rho_s^{(a/b)}(t), \alpha), \tag{35}$$

where a and b are chosen for outgoing and ingoing roads at the junction, respectively. For the above formulas, let us assume that road j connects two junctions.

Hence, Eqs. (30)–(35) define a closed system of coupled ODEs. To solve, we discretize (30)–(35) using a fixed step-width τ. The discretized equations for the ODE model for a road j are given by following system of coupled equations:

$$\rho_j^{(a)}(t + \tau) = \rho_j^{(a)}(t) - \frac{2\tau}{L}\left(f\left(\frac{\rho_j^{(a)}(t) + \rho_j^{(b)}(t)}{2}\right) - f(\overline{\rho}_j^a(t))\right), \tag{36}$$

$$\rho_j^{(b)}(t + \tau) = \rho_j^{(b)}(t) + \frac{2\tau}{L}\left(f\left(\frac{\rho_j^{(a)}(t) + \rho_j^{(b)}(t)}{2}\right) - f(\overline{\rho}_j^b(t))\right), \tag{37}$$

$$\overline{\rho}_j^a(t) = U_a^j(\rho_j^{(a)}(t), \rho_k^{(a/b)}(t), \rho_l^{(a/b)}(t)), \tag{38}$$

$$\overline{\rho}_j^b(t) = U_b^j(\rho_j^{(b)}(t), \rho_r^{(a/b)}(t), \rho_s^{(a/b)}(t), \alpha). \tag{39}$$

Of course, τ should satisfy the CFL condition [22], since the above discretization can be seen as finite-difference scheme for a conservation law, i.e., we require τ to fulfill the following condition:

$$\tau \leqslant \frac{L}{2 \max_\rho f'(\rho)}. \tag{40}$$

In the numerical results we will see that the naive discretization by an explicit Euler-scheme as in (36), (37) does not produce comparable results to a Godunov-discretization of (5). Indeed, it is well-known that this scheme is oscillating. Therefore, we propose a Lax–Friedrichs [22] discretization of the time derivative, i.e., of Eqs. (30) and (31). Finally, we obtain the following system (ODE model) for a road j connected to two junctions and τ as in (40).

$$\rho_j^{(a)}(t+\tau) = \left(\frac{\overline{\rho}_j^a(t) + \rho_j^{(b)}(t)}{2} \right) - \frac{2\tau}{L}(f(\rho_j^{(b)}(t)) - f(\overline{\rho}_j^a(t))), \tag{41}$$

$$\rho_j^{(b)}(t+\tau) = \left(\frac{\rho_j^{(a)}(t) + \overline{\rho}_j^b(t)}{2} \right) + \frac{2\tau}{L}(f(\rho_j^{(a)}(t)) - f(\overline{\rho}_j^b(t))), \tag{42}$$

$$\overline{\rho}_j^a(t) = U_a^j(\rho_j^{(a)}(t), \rho_k^{(a/b)}(t), \rho_l^{(a/b)}(t)), \tag{43}$$

$$\overline{\rho}_j^b(t) = U_b^j(\rho_j^{(b)}(t), \rho_r^{(a/b)}(t), \rho_s^{(a/b)}(t), \alpha). \tag{44}$$

Remark 3. Note that (41)–(44) is different from any discretization of the partial differential equation (5) due to the approximation of $\rho_j(d, t)$ in (32) and due to the definition of the boundary values $\overline{\rho}_j^{a,b}(t)$.

The ODE model (41)–(44) uses functions $U_{a,b}^j(\cdot)$ of the PDE model. Hence, also the ODE model inherits the property of traffic jams moving backwards through the junction as explained in Remark 2.

3. Optimization problems

We consider optimization problems governed by the ODE model introduced above. We assume in the following that traffic can be distributed at certain dispersing junctions of the network. In terms of our model, we have a percentage $0 \leqslant \alpha_i \leqslant 1$ for each dispersing junction $i = 1, \ldots, n$. In practical applications, the value of α_i is a recommendation and might be given for example by detour suggestions in the car-navigation systems or signs at the corresponding highway intersections. For simplicity, we assume that the traffic is actually distributed according to the value of α_i. Of course, there are situations where not all cars follow the recommendations and a more sophisticated model has to take into account random behaviour at the junction. Nevertheless, the discussion below is interesting for traffic management and investigations of "optimal" utilization of a given network.

In the following, we assume a network geometry with one inflow and one outflow arc. Further, the inflow profile $\rho_0(t)$ and a time horizon $T > 0$ is given. At each dispersing junction $i = 1, \ldots, n$ of the network we apply a control $\alpha_i \in [0, 1]$ which appears in the function U_b^j and control the distribution of the flux on the outgoing roads.

A measure for the utilization of a single road j of the network is the time and space averaged density $\int_0^T \int_{a_j}^{b_j} \rho(x, t)\, \mathrm{d}x\, \mathrm{d}t$. Hence, an objective functional is

$$J_2(\vec{\alpha}; T, \rho_0) = \sum_{j=1}^{I} \int_0^T \int_a^b \rho_j(x, t)\, \mathrm{d}x\, \mathrm{d}t. \tag{45}$$

It is easy to verify that in case of a single inflow arc j_0 and outflow arc j_I and sufficiently regular solutions ρ_j

$$J_2(\vec{\alpha}; T, \rho_0) = \int_0^T f_{j_0}(\rho(a_{j_0}, t))\, \mathrm{d}t - \int_0^T f_{j_I}(\rho(b_j, t))\, \mathrm{d}t. \tag{46}$$

We are interested in controls $\vec{\alpha}$ such that the functional $J_2(\vec{\alpha})$ is minimized and give the precise optimization problem below.

Remark 4. The functional $J_2(\vec{\alpha}; T, \rho_0)$ is popular in the traffic engineering community [20,21]. According to (46), it measures the possible maximal flow passing the network depending on routing decisions at junctions. Since the flux functions are concave, high densities are related to small velocities v_j, i.e., $\rho_j v_j = f_j(\rho_j)$. Therefore, minimizing (45) yields a traffic situation with a large average speed. Similarly, the functional J_2 penalizes backward moving waves in the network. These waves can be interpreted as traffic jams.

To obtain an approximation of J_2 for the ODE model of the previous sections, we consider the discretized and space averaged objective function J_{2t}, i.e.,

$$J_{2t}(\alpha; T, \rho_0) = \sum_{t=1}^{T} \sum_{j=1}^{I} \frac{L_j}{2} \tau(\rho_j^{(a)}(t) + \rho_j^{(b)}(t)) \tag{47}$$

and the minimization problem

$$\min_{\vec{\alpha}} J_{2t} \quad \text{s.t. } 0 \leqslant \alpha_i \leqslant 1, \ i = 1, \ldots, n \ \text{ and } \ (41)\text{–}(44). \tag{48}$$

3.1. Adjoint and gradient equation

We derive the optimality conditions for (48) in this section. The gradient and adjoint equation are used in the numerical solution of (48) later on. To avoid superfluous notations we consider a general minimization problem (49) governed by ODEs first and then state the result for (48).

The general calculus [4] considers the problem

$$\min_{\alpha \in \mathbb{R}^n} f(\alpha) \quad \text{s.t. } (50) \tag{49}$$

wherein the state equation is given by

$$y_t = F_t(y_{t-1}, \alpha) \quad \text{for } t = 1, \ldots, T \tag{50}$$

and y_0 given. For each t, F_t is a differentiable, non-linear function from $\mathbb{R}^m \times \mathbb{R}^n$ to $\mathbb{R}^m$. Further the differentiable objective function, $f : \mathbb{R}^m \times \mathbb{R}^n \to \mathbb{R}$, has the following form:

$$f = \sum_{t=1}^{T} f_t(y_t, \alpha). \tag{51}$$

The optimality system can be derived as follows. Let $g_t \in \mathbb{R}^n$ be the gradient of f as a function of control variables α. To obtain g_t, we differentiate (50) and use the differentials $u = \mathrm{d}\alpha \in \mathbb{R}^n$, $z = \mathrm{d}y \in \mathbb{R}^m$

$$z_t = (F_t)'_y(y_{t-1}, \alpha) z_{t-1} + (F_t)'_\alpha(y_{t-1}, \alpha) u_t, \quad z_0 = 0. \tag{52}$$

By (51)

$$\mathrm{d}f = \sum_{t=1}^{T} (\nabla_y f_t(y_t, u_t), z_t)_m + \sum_{t=1}^{T} (\nabla_\alpha f_t(y_t, u_t), u_t)_n. \tag{53}$$

To obtain the adjoint equation we eliminate z as follows:

(1) Setting $G_t = (F_t)'_y(y_{t-1}, \alpha)$, $H_t = (F_t)'_\alpha(y_{t-1}, \alpha)$, $\gamma_t = \nabla_y f_t(y_t, u_t)$ and $h_t = \nabla_\alpha f_t(y_t, u_t)$. Multiply each linearized state equation in (52) by a vector $p_t \in \mathbb{R}^m$ and summing up we have

$$0 = -(p_T, z_T) + \sum_{t=1}^{T-1} (p_t, z_t)_m + \sum_{t=1}^{T-1} (G_{t+1}^\top p_{t+1}, z_t)_m + \sum_{t=1}^{T} (H_t^\top p_t, u_t)_n. \tag{54}$$

(2) Adding this to the expression of $\mathrm{d}f$,

$$\mathrm{d}f = (-p_T + \gamma_T, z_T)_m + \sum_{t=1}^{T-1} (-p_t + G_{t+1}^\top p_{t+1} + \gamma_t, z_t)_m + \sum_{t=1}^{T} (H_t^\top p_t + h_t, u_t)_n. \tag{55}$$

(3) Choosing p such that coefficients of z_t vanish

$$p_T = \gamma_T, \quad p_t = G_{t+1}^{\top} p_{t+1} + \gamma_t \quad \text{for } t = T-1, \dots, 1. \tag{56}$$

Then we obtain the gradient in desired form

$$g_t = H_t^{\top} p_t + h_t \quad \text{for } t = 1, \dots, T. \tag{57}$$

Eq. (56) is called the *adjoint equation* and Eq. (57) is called the *gradient equation*.

We apply the general discussion to the minimization problem (48). Considering the ODE-model (41)–(44) and the objective functional (47), we denote by

$$y_t^j = \begin{pmatrix} \rho_j^{(a)}(t) \\ \rho_j^{(b)}(t) \end{pmatrix} = \begin{pmatrix} y_t^{1,j} \\ y_t^{2,j} \end{pmatrix} \quad \forall j = 1, \dots, I. \tag{58}$$

Hence, $m = 2I$, where I is the number of roads and n is the number of dispersing junctions in the network. Therefore, the control variable $\alpha \in \mathbb{R}^n$ and the state variables $y_t \in \mathbb{R}^m$ for each t.

We rewrite (41)–(44) as

$$\begin{aligned} y_t^{1,j} &= F_t^{1,j}(y_{t-1}^{1,j}, y_{t-1}^{2,j}, \alpha), \\ y_t^{2,j} &= F_t^{2,j}(y_{t-1}^{1,j}, y_{t-1}^{2,j}, \alpha), \\ y_t^{j} &= F_t^{j}(y_{t-1}^{j}, \alpha) \quad \text{for } t = 1, \dots, T. \end{aligned} \tag{59}$$

We apply the abstract calculus introduced above and compute the derivatives, G_t, H_t, γ_t and h_t as follows. We discuss the non-zero elements in G_t. The block in G_t corresponding to ingoing road 1 and outgoing road I is

$$(G_{t+1})_1 = \left[0 \quad \left(\frac{1}{2} - \frac{2\tau}{L} f_1'(\rho_1^{(b)}(t)) \right) \right], \tag{60}$$

$$(G_{t+1})_{2I} = \left[\left(\frac{1}{2} + \frac{2\tau}{L} f_I'(\rho_I^{(a)}(t)) \right) \quad \left(\frac{1}{2} - \frac{2\tau}{L} f_I'(\rho_I^{(b)}(t)) \right) \right]. \tag{61}$$

The block corresponding to the road j as in Fig. 1 is

$$(G_{t+1})_{2j-1,2j} = \begin{bmatrix} \left(\frac{1}{2} + \frac{2\tau}{L} f_j'(\overline{\rho}_j^a(t)) \right) \frac{\partial \overline{\rho}_j^a(t)}{\partial \rho_{j,k,l}^{(a)}(t)} & \frac{1}{2} - \frac{2\tau}{L} f_j'(\rho_j^b(t)) \\ \frac{1}{2} + \frac{2\tau}{L} f_j'(\rho_j^a(t)) & \left(\frac{1}{2} - \frac{2\tau}{L} f_j'(\overline{\rho}_j^b(t)) \right) \frac{\partial \overline{\rho}_j^b(t)}{\partial \rho_{j,r,s}^{(b)}(t)} \end{bmatrix}. \tag{62}$$

The non-zero elements of H_t are given by

$$(H_t)_{ji} = \begin{bmatrix} \left(\frac{1}{2} + \frac{2\tau}{L} f_j'(\overline{\rho}_j^a) \right) \frac{\partial \overline{\rho}_j^a}{\partial \alpha_i} \\ \left(\frac{1}{2} - \frac{2\tau}{L} f_j'(\overline{\rho}_j^b) \right) \frac{\partial \overline{\rho}_j^b}{\partial \alpha_i} \end{bmatrix}. \tag{63}$$

The derivatives of objective functional J_{2t} are given by following formulas:

$$\gamma_t = \nabla_y J_{2t} = \frac{b-a}{2} \tau [1]_{m \times 1}, \tag{64}$$

$$h_t = \nabla_{\alpha_i} J_{2t} = [0]_{n \times 1}. \tag{65}$$

It remains to discuss derivatives with respect to the boundary controls $U_{a,b}^j$. We distinguish the dispersing and merging junction according to the discussion in the previous sections. Due to the possibility of backward moving waves, the derivatives are discontinuous.

For dispersing junction with control parameter α_i, incoming road 1 and outgoing roads 2, 3 we have

$$\nabla U^1(\rho_1^{(b)},\rho_2^{(a)},\rho_3^{(a)},\alpha_i)=\left(\begin{bmatrix}1 & \gamma=c_1,\ \rho_1^{(b)}<\sigma_1\\ 0 & \text{else}\end{bmatrix},\begin{bmatrix}d_{\rho_2^{(a)}}f_1^{-1,+}\left(\frac{1}{\alpha_i}f_2(\rho_2^{(a)})\right) & \gamma=\frac{c_2}{\alpha_i},\ \rho_2^{(a)}>\sigma_2\\ 0 & \text{else}\end{bmatrix},\right.$$

$$\left.\begin{bmatrix}d_{\rho_3^{(a)}}f_1^{-1,+}\left(\frac{1}{1-\alpha_i}\,f_3(\rho_3^{(a)})\right) & \gamma=\frac{c_3}{1-\alpha_i},\ \rho_3^{(a)}>\sigma_3\\ 0 & \text{else}\end{bmatrix},\begin{bmatrix}0 & \gamma=c_1\\ d_{\alpha_i}f_1^{-1,+}\left(\frac{1}{\alpha_i}c_2\right) & \gamma=\frac{c_2}{\alpha_i}\\ d_{\alpha_i}f_1^{-1,+}\left(\frac{1}{1-\alpha_i}c_3\right) & \gamma=\frac{c_3}{1-\alpha_i}\end{bmatrix}\right),$$

$$\nabla U^2(\rho_1^{(b)},\rho_2^{(a)},\rho_3^{(a)},\alpha_i)=\left(\begin{bmatrix}d_{\rho_1^{(b)}}f_2^{-1,-}(\alpha_i f_1(\rho_1^{(b)})) & \gamma=c_1,\ \rho_1^{(b)}<\sigma_1\\ 0 & \text{else}\end{bmatrix},\right.$$

$$\left.\begin{bmatrix}1 & \gamma=\frac{c_2}{\alpha_i},\ \rho_2^{(a)}>\sigma_2\\ 0 & \text{else}\end{bmatrix},\begin{bmatrix}d_{\rho_3^{(a)}}f_2^{-1,-}\left(\frac{\alpha_i}{1-\alpha_i}f_3(\rho_3^{(a)})\right) & \gamma=\frac{c_3}{1-\alpha_i},\ \rho_3^{(a)}>\sigma_3\\ 0 & \text{else}\end{bmatrix},\begin{bmatrix}d_{\alpha_i}f_2^{-1,-}(\alpha_i c_1) & \gamma=c_1\\ 0 & \gamma=\frac{c_2}{\alpha_i}\\ d_{\alpha_i}f_2^{-1,-}\left(\frac{\alpha_i}{1-\alpha_i}\,c_3\right) & \gamma=\frac{c_3}{1-\alpha_i}\end{bmatrix}\right),$$

$$\nabla U^3(\rho_1^{(b)},\rho_2^{(a)},\rho_3^{(a)},\alpha_i)=\left(\begin{bmatrix}d_{\rho_1^{(b)}}f_3^{-1,-}((1-\alpha_i)f_1(\rho_1^{(b)})) & \gamma=c_1,\ \rho_1^{(b)}<\sigma_1\\ 0 & \text{else}\end{bmatrix},\right.$$

$$\left.\begin{bmatrix}d_{\rho_2^{(a)}}f_3^{-1,-}\left(\frac{1-\alpha_i}{\alpha_i}\,f_2(\rho_2^{(a)})\right) & \gamma=\frac{c_2}{\alpha_i},\ \rho_2^{(a)}>\sigma_2\\ 0 & \text{else}\end{bmatrix},\begin{bmatrix}1 & \gamma=\frac{c_3}{1-\alpha_i},\ \rho_3^{(a)}>\sigma_3\\ 0 & \text{else}\end{bmatrix},\begin{bmatrix}d_{\alpha_i}f_3^{-1,-}((1-\alpha_i)c_1) & \gamma=c_1\\ d_{\alpha_i}f_3^{-1,-}\left(\frac{1-\alpha_i}{\alpha_i}c_2\right) & \gamma=\frac{c_2}{\alpha_i}\\ 0 & \gamma=\frac{c_3}{1-\alpha_i}\end{bmatrix}\right).$$

For a junction where roads 1 and 2 merge in road 3, we obtain

$$\nabla U^1(\rho_1^{(b)},\rho_2^{(b)},\rho_3^{(a)}) = \left(\begin{bmatrix} 1 & \gamma = c_1,\ \rho_1^{(b)} < \sigma_1 \\ 0 & \text{else} \end{bmatrix}, \begin{bmatrix} d_{\rho_2^{(b)}} f_1^{-1,+}(f_2(\rho_2^{(b)})) & \gamma = c_2,\ \rho_2^{(b)} < \sigma_2 \\ 0 & \text{else} \end{bmatrix}, \begin{bmatrix} d_{\rho_3^{(a)}} f_1^{-1,+}\left(\dfrac{f_3(\rho_3^{(a)})}{2}\right) & \gamma = \dfrac{c_3}{2},\ \rho_3^{(a)} > \sigma_3 \\ 0 & \text{else} \end{bmatrix}\right),$$

$$\nabla U^2(\rho_1^{(b)},\rho_2^{(b)},\rho_3^{(a)}) = \left(\begin{bmatrix} d_{\rho_1^{(b)}} f_2^{-1,+}(f_1(\rho_1^{(b)})) & \gamma = c_1,\ \rho_1^{(b)} < \sigma_1 \\ 0 & \text{else} \end{bmatrix}, \begin{bmatrix} 1 & \gamma = c_2,\ \rho_2^{(b)} < \sigma_2 \\ 0 & \text{else} \end{bmatrix}, \begin{bmatrix} d_{\rho_3^{(a)}} f_2^{-1,+}\left(\dfrac{f_3(\rho_3^{(a)})}{2}\right) & \gamma = \dfrac{c_3}{2},\ \rho_3^{(a)} > \sigma_3 \\ 0 & \text{else} \end{bmatrix}\right).$$

For ∇U^3 we need to consider two cases: if $c_1 + c_2 \leqslant c_3$ then $\gamma_3 = c_1 + c_2$ and the gradient is given by

$$\nabla U^3(\rho_1^{(b)},\rho_2^{(b)},\rho_3^{(a)}) = (d_{\rho_1^{(b)}} f_3^{-1,-}(f_1(\rho_1^{(b)}) + f_2(\rho_2^{(b)})), d_{\rho_2^{(b)}} f_3^{-1,-}(f_1(\rho_1^{(b)}) + f_2(\rho_2^{(b)})),$$
$$d_{\rho_3^{(a)}} f_3^{-1,-}(f_1(\rho_1^{(b)}) + f_2(\rho_2^{(b)})) = 0).$$

On the other hand, if $\gamma_3 = \min(c_1, c_2, c_3/2)$ then the gradient is given by

$$\nabla U^3(\rho_1^{(b)},\rho_2^{(b)},\rho_3^{(a)}) = \left(\begin{bmatrix} d_{\rho_1^{(b)}} f_3^{-1,-}(f_1(\rho_1^{(b)})) & \gamma = c_1,\ \rho_1^{(b)} < \sigma_1 \\ 0 & \text{else} \end{bmatrix}, \begin{bmatrix} d_{\rho_2^{(b)}} f_3^{-1,-}(f_2(\rho_2^{(b)})) & \gamma = c_2,\ \rho_2^{(b)} < \sigma_2 \\ 0 & \text{else} \end{bmatrix}, \begin{bmatrix} 1 & \gamma = \dfrac{c_3}{2},\ \rho_1^{(a)} > \sigma_3 \\ 0 & \text{else} \end{bmatrix}\right).$$

This finishes the discussion of gradient and adjoint equations for the ODE-model (41)–(44) and the optimization problem (48).

Remark 5. We give an example for the flux function $f_j(\rho_j) = 4\rho_j(1 - \rho_j/\rho_j^{\max})$,

$$d_{\rho_k} f_l^{-1,\pm}(v(\alpha_i)\cdot f_k(\rho_k)) = \frac{\mp 1}{4}\left(\frac{M_l v(\alpha_i)\cdot f_k'(\rho_k)}{\sqrt{M_l^2 - M_l.v(\alpha_i)\cdot f_k(\rho_k)}}\right), \tag{66}$$

$$d_{\alpha_i} f_l^{-1,\pm}(v(\alpha_i)c_k) = \frac{\mp 1}{4}\,\frac{M_l \partial_{\alpha_i} v(\alpha_i)c_k}{\sqrt{M_l^2 - M_l v(\alpha_i)c_k}}, \tag{67}$$

where

$$\partial_{\alpha_i} v(\alpha_i) = \begin{bmatrix} 1 & \text{if } \alpha_i \\ -1 & \text{if } 1-\alpha_i \\ \dfrac{-1}{\alpha_i^2} & \text{if } \dfrac{1}{\alpha_i} \text{ or } \dfrac{1-\alpha_i}{\alpha_i} \\ \dfrac{1}{(1-\alpha_i)^2} & \text{if } \dfrac{1}{1-\alpha_i} \text{ or } \dfrac{\alpha_i}{1-\alpha_i} \end{bmatrix}. \tag{68}$$

4. Numerical results

If not stated otherwise we assume the following setting for our numerical examples:

$$f_j(\rho_j) = 4\rho_j(1-\rho_j/M_j), \quad M_j = 1, \quad L_j = 1, \quad \sigma_j = M_j/2, \quad T = 5, \quad \rho_{j,0} = 0.$$

Herein, M_j is the maximal density on road j, i.e., $M_j = \rho_j^{\max}$. The step-width of the time-discretization τ in the ODE models (36)–(39) and (41)–(44) is set to $\tau = \frac{1}{10}$.

The PDE-model (26)–(29) is discretized using a first-order Godunov-scheme on an equidistant grid with $N_x \times N_t$ gridpoints. The objective functional J_2 is discretized using a trapezoidal rule with equidistant spacing.

4.1. Comparison of the ODE-model (36)–(39) and (41)–(44)

We consider the situation at a single junction of either dispersing or merging type. In case of a dispersing junction we fix $\alpha = \frac{3}{10}$ and consider a constant inflow $\rho_0 = 0.3$. The results are given in Figs. 2 and 4. In case of merging junction we have choosen inflow $\rho_0 = 0.1$, on both incoming roads and present results in Figs. 3 and 5. We observe an unphysical bump on the outgoing roads of the dispersing and merging junction in the case of model (36)–(39). The bump is not present in the (modified) model (41)–(44). In this case we observe a smooth transition profile through the junction. Since the outgoing roads are initially empty, this is to be expected (Figs. 2–5).

4.2. Comparison of the ODE (41)–(44) and PDE model (26)–(29) on a sample network

In this section, we compare the PDE and ODE models on a sample network. We plot contour lines for J_2 and J_{2t} objective functional for both models for the sample network in Fig. 6. The sample network has two controls α_1 and α_2, hence the objective functional J_2 and J_{2t} can be computed for all possible combinations of controls. This allows

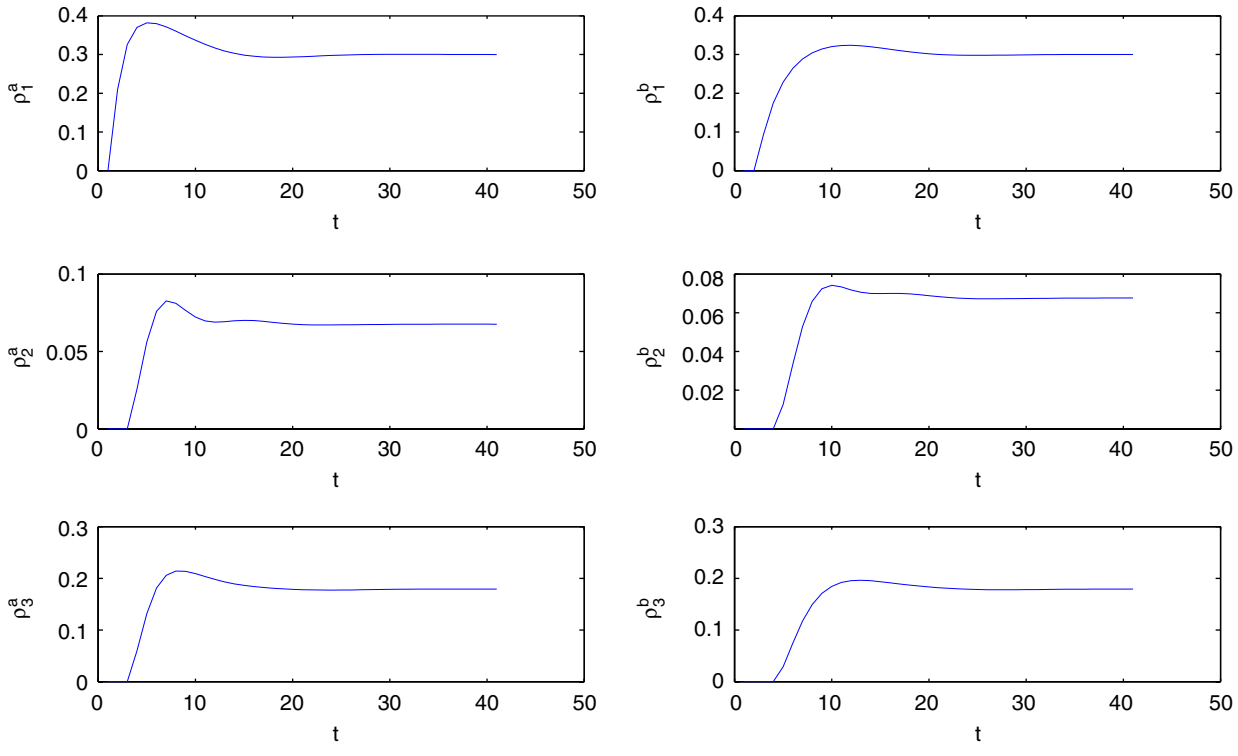

Fig. 2. Dispersing junction (ODE model (36)–(39)).

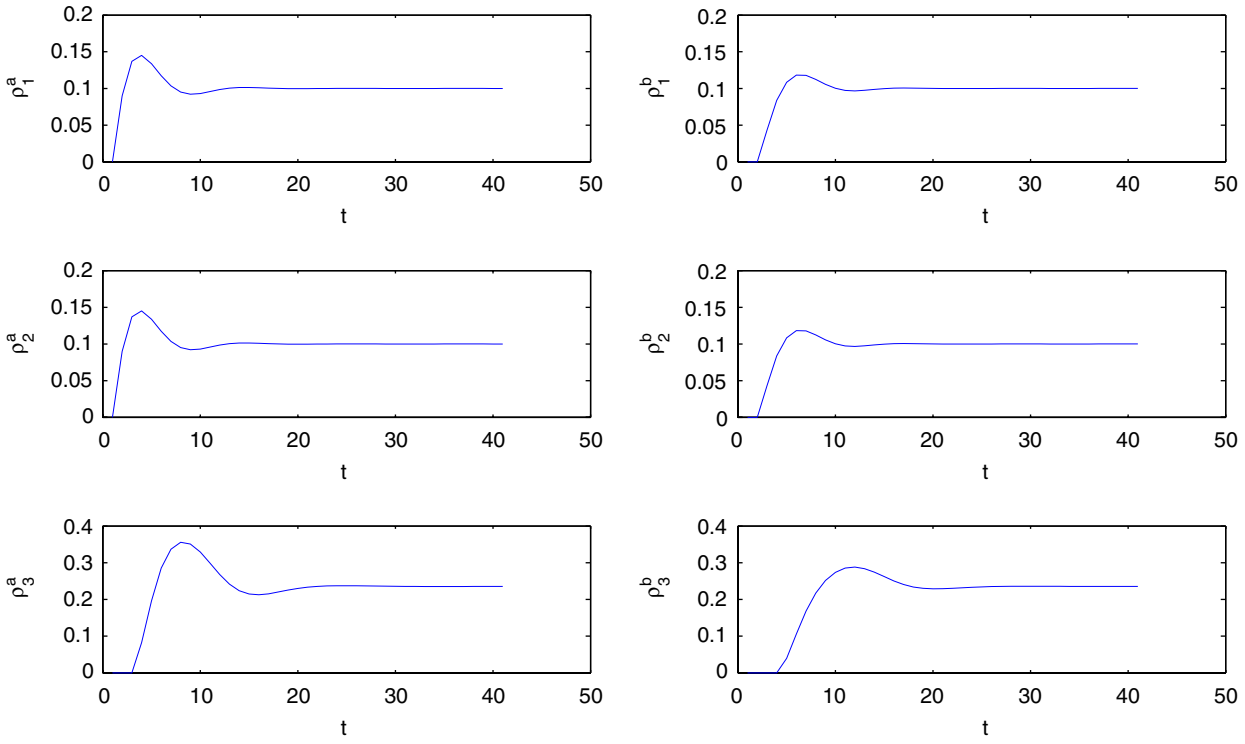

Fig. 3. Merging junction (ODE model (36)–(39)).

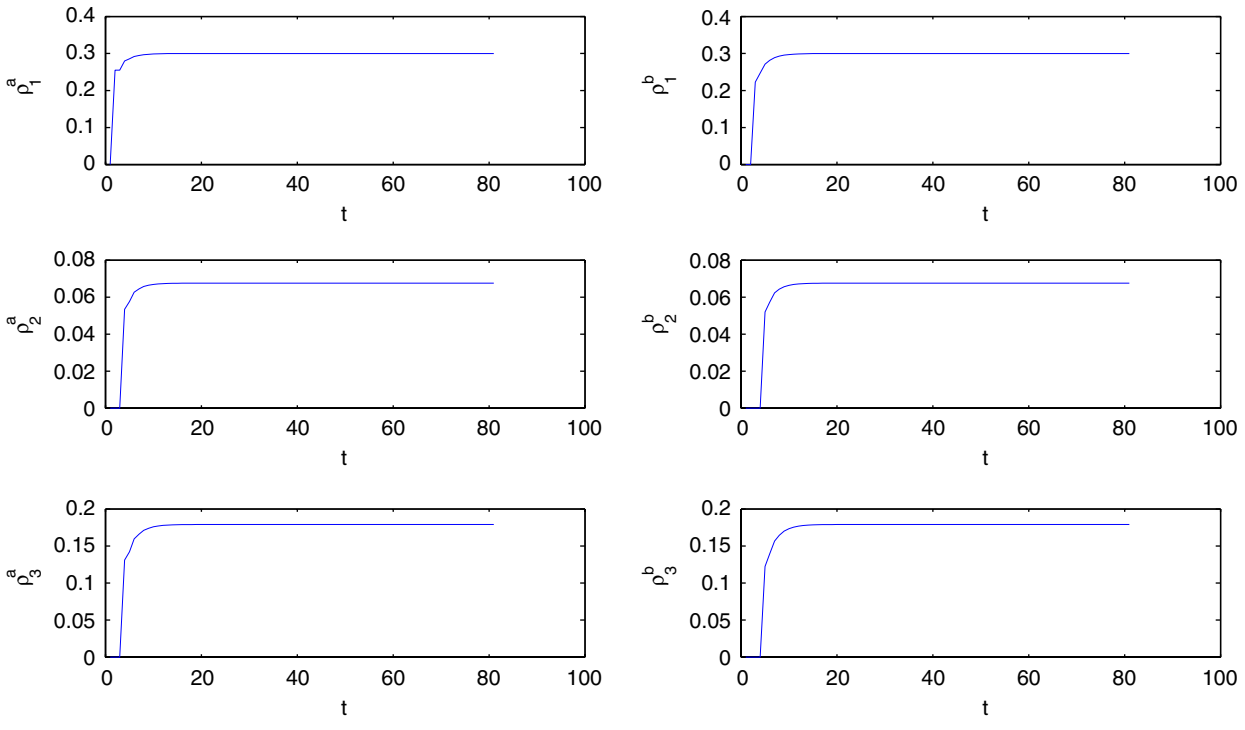

Fig. 4. Dispersing junction (ODE model (41)–(44)).

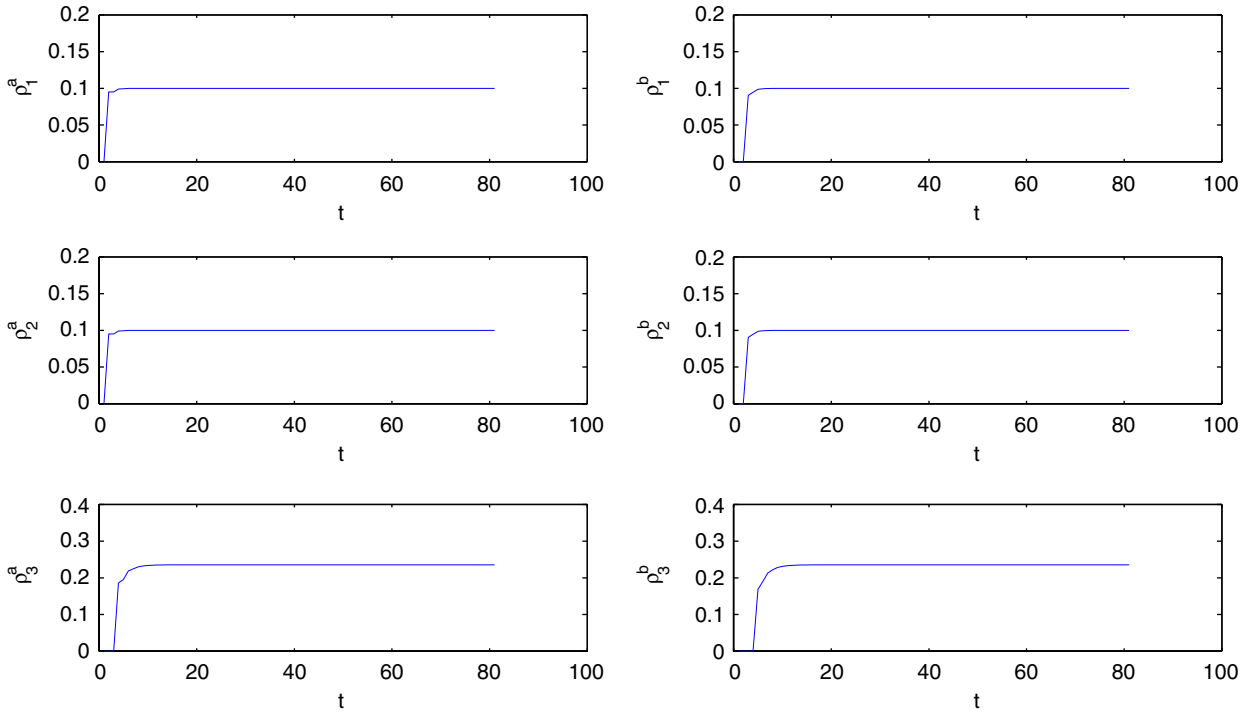

Fig. 5. Merging junction (ODE model (41)–(44)).

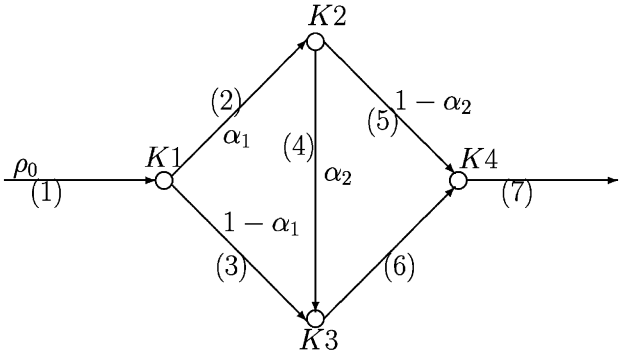

Fig. 6. Sample network.

to investigate if the ODE model (41)–(44) has similar properties than the full PDE-model. We consider two different situations corresponding to a free-flow and a traffic jam situation. In the free-flow case, the inflow on road 1 is given by $f_1(\rho_0) = 96\%$ and less than the capacity $M_j = 1$ of each road j. Therefore, no traffic jam can occur independent of the applied controls (α_1, α_2). The contour plots of the objective functionals are given in Fig. 7. We observe a qualitative correspondence of both models and note that even the optimal controls $(\frac{1}{2}, 0)$ coincide in this case. Next, we consider a situation of congested network by varying the maximal densities on each road. We model this by a reduction of the maximal density and set $M_1 = M_2 = M_4 = M_6 = M_7 = 2$, $M_3 = 1$ and $M_5 = 0.5$. The inflow is again $f_1(\rho_0) = 96\%$. The contour lines of functionals J_2 and J_{2t} are given in Fig. 8. The white parts of the plot show correspond to controls (α_1, α_2), where a traffic jam reached the inflow arc. Those traffic jams appear in both the ODE and the PDE model for $\alpha_1 \leqslant 46\%$. Additionally, the PDE model simulates those jams for $\alpha_1 > 90\%$ in contrast to $\alpha_1 > 95\%$ for the ODE model. For the remaining controls we observe a very similar behaviour.

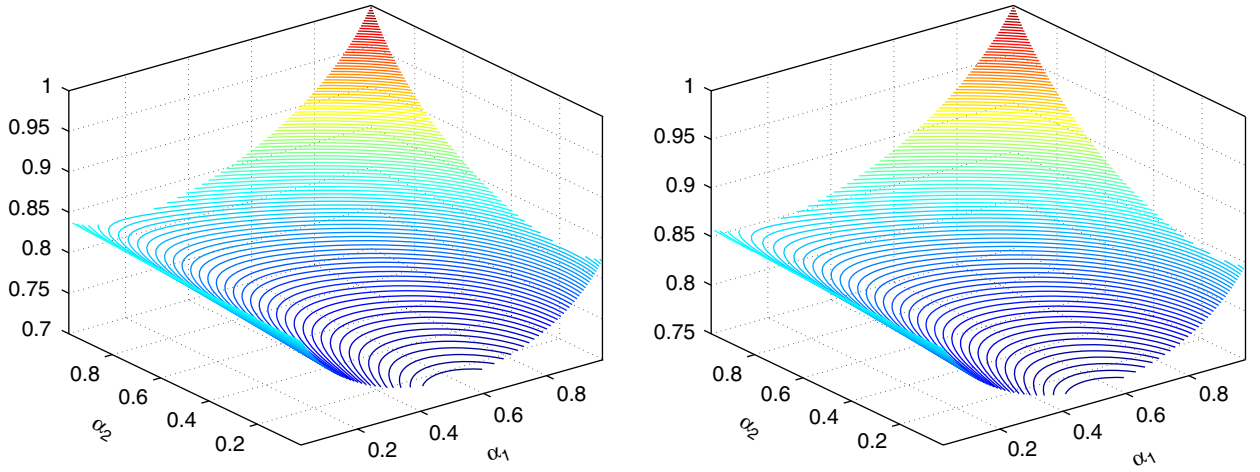

Fig. 7. Contour lines of cost functional J_{2t}, J_2 for ODE (left) and PDE (right) model, respectively.

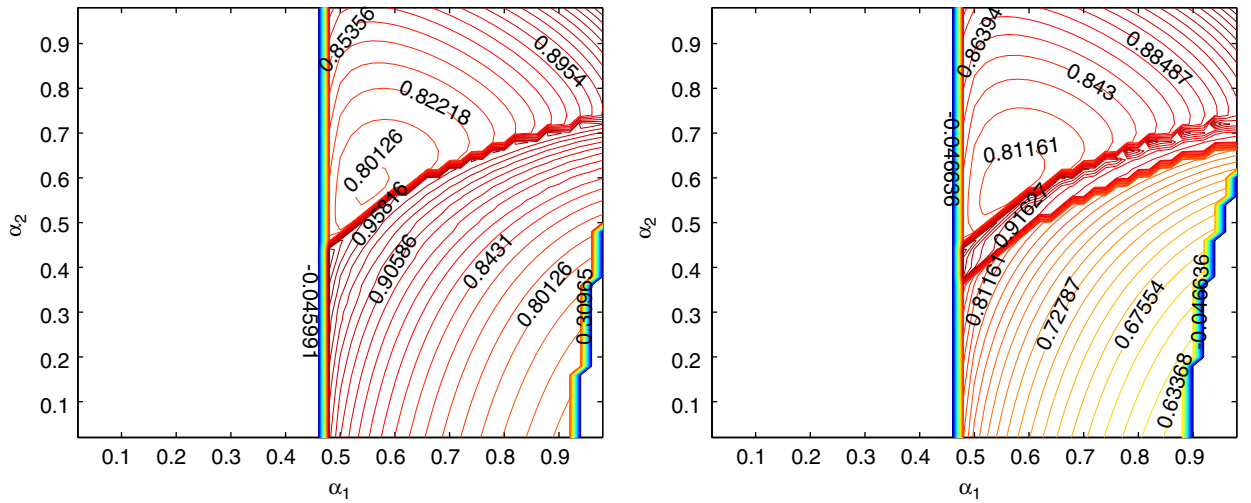

Fig. 8. Contour lines of J_{2t} and J_2 objective functionals for ODE (left) and PDE (right) model with occurrence of congestions.

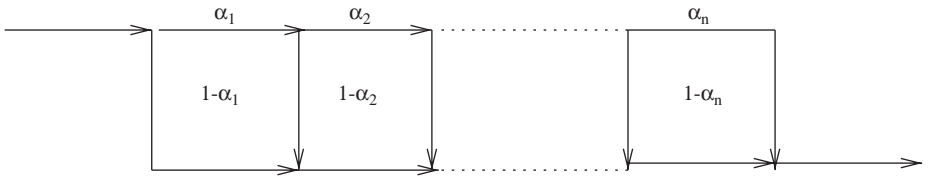

Fig. 9. Layout of a scalable network.

4.3. Comparison of CPU times

Besides the qualitative comparison given in the previous section, we present computational results. We consider a scalable network as in Fig. 9 with n controls α_i $i = 1, \ldots, n$ in the top row and a total of $3n - 1$ roads. We assume a constant inflow, fix a time $T > 0$ and values for controls α_i. We measure the CPU-time needed for the computation of

Table 1
CPU times in seconds for both models on networks of different sizes

No. of roads	ODE model	PDE model
7	0.01	0.929
31	0.33	8.98
61	1.07	29.82

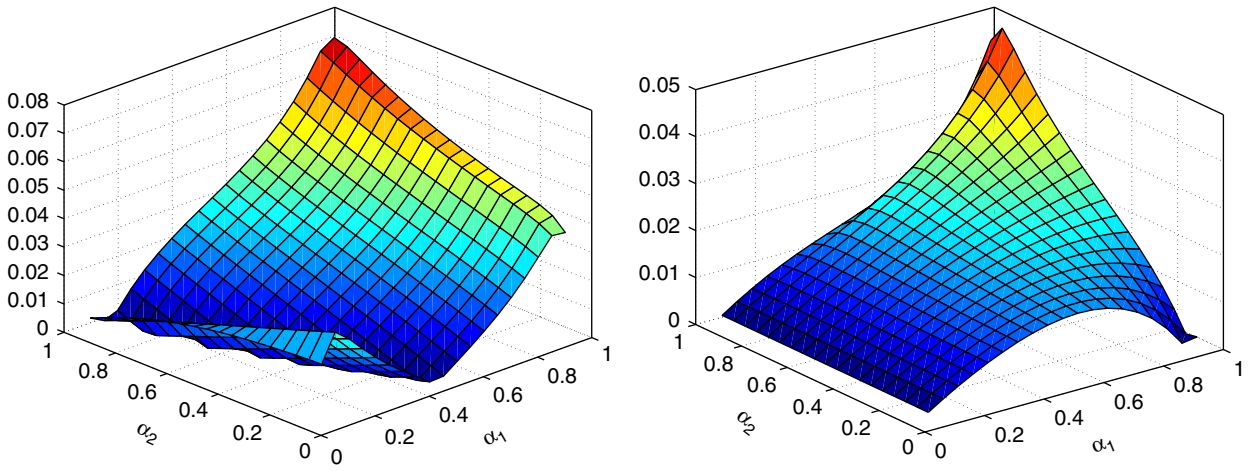

Fig. 10. Difference of adjoint gradient and finite difference approximation gradients.

the ODE model (41)–(44) and compare with the CPU-time needed for the computation of the PDE model (26)–(29). The comparison depends upon the number of discretization points used for the Godunov scheme and on the size of the network. We present in Table 1 results for a space discretization with $N_x = 100$ gridpoints per each road and networks of the sizes 7–61. All computations are performed on a 1.8 GHz Intel Pentium M under Matlab V6R13. The CPU times for the PDE are a factor 9–30 larger than those for the ODE and the difference increases with the size of the network. This is a severe drawback of the PDE model if we focus on optimization problems, where we need to solve the PDE in each iteration of the optimization (probably more than once).

4.4. Gradient information

We consider the network of Fig. 7. Gradients for the functional J_{2t} and (41)–(44) can be obtained either by using the discrete adjoint equations of Section 3.1 or by a finite difference approximation for J_{2t} using (41)–(44).

For each control α_1 and α_2 we proceed as follows. We fix $\tau = \frac{1}{10}$. We compute finite differences by one-sided differences with $\Delta\alpha_i = 10^{-1}$. For comparison, we compute the adjoints and the gradient by the calculus in Section 3.1. We plot the absolute difference between both in Fig. 10. The gradients differ in order $O(\Delta\alpha_i)$ and vanish at the optimal values $(\frac{1}{2}, 0)$.

Of course, there is major advantage of using the adjoint calculus instead of finite differences. The adjoint calculus yields all derivatives after single computation of (56) and (57); whereas for finite differences we have to compute (41)–(44) for each control α_i at least twice.

4.5. Optimization results

We consider the numerical solution of (48). This problem is a non-convex, box and equality constrained optimization problem. By the adjoint calculus of Section 3.1 we have exact gradients for the reduced objective functional at hand. This allows to apply general methods for box-constrained optimization. We consider different descent methods for

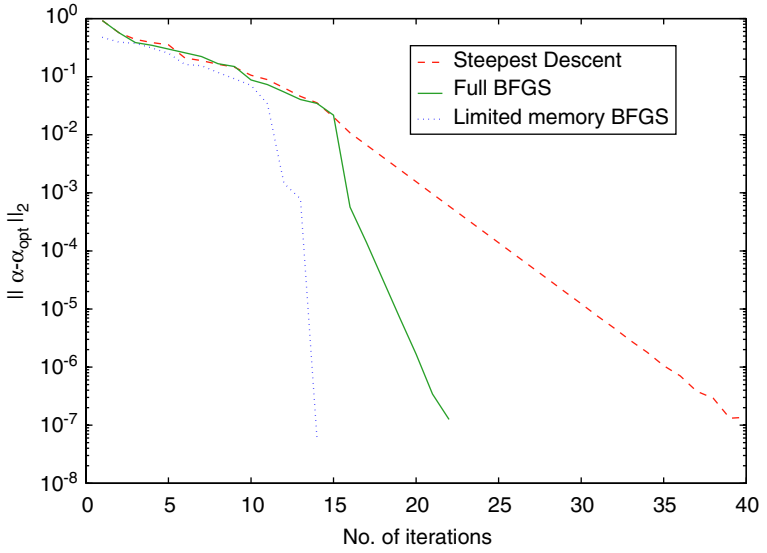

Fig. 11. Convergence results for larger networks.

solving (48). For a comparison, we use a simple steepest descent and incorporate the box constraints by projection. The step-width is choosen according to the Armijo-rule [17]. Fast convergence is expected and observed (see Fig. 11). The full BFGS method is quasi-Newton method and determines approximations to the Hessian of the Lagrangian by the BFGS update formula [17,26]. We combine the general BFGS with an active set strategy as in [17,3,7] and use the Armijo step-width rule to satisfy the sufficient decrease condition. Especially, for large networks it is not possible to store an approximation of the full Hessian. Therefore, we apply the state-of-the-art L-BFGS-B code by [6,27]. This code implements a projected gradient method with a limited memory BFGS update and performs well compared with other optimization methods, see [6] and references therein.

Note that due to the lack of second-order information on the problem, we cannot expect quadratic convergence results. If we apply quasi-Newton-type methods we can achieve super-linear convergence, see [4,17,26] for a more detailed discussion.

Other numerical optimization methods like for example SQP trust-region [9] methods, augmented Lagrangian methods or penalty methods [2] can also be applied in this context. A comparison to those methods is still under investigation.

For a comparison of the performance of the several optimization methods, we consider the academic network of Fig. 9. The reason for choosing this network instead of a more realistic one is that we know the optimal controls α_i in this particular case. For a constant inflow $f_1(\rho_0)$ and T sufficiently large and $L_j = b_j - a_j = 1$ the optimal controls are $\alpha = (\frac{1}{2}, 1, \ldots, 1)$, i.e., the flow is such that all roads connecting top and bottom row remain empty. Therefore, we can plot for each iteration step of a numerical optimization method the L^2-norm of the residual. We report results for a network with 20 controls and 61 streets in Fig. 11.

The major highway network in southern Germany has a structure as in Fig. 11 with a total of 10 roads. We are currently collecting data of a major German highway network to obtain realistic initial conditions and inflow profiles. This will be presented in a forthcoming work.

5. Conclusion

Starting from a macroscopic traffic model for flows on networks, we derived a model based on ODEs. This model enjoys similar qualitative properties than the full model but is cheaper in terms of computational time. We study optimization problems governed by the introduced model and derived a adjoint calculus. We presented numerical results on sample networks and leave the application to real-world data for future work.

Results suggest that the proposed model is computationally cheap, contains reasonable approximations of the traffic behaviour given by the full model and can be used for optimization issues in traffic management.

References

[1] A. Aw, M. Rascle, Resurrection of second order models of traffic flow?, SIAM J. Appl. Math. 60 (2000) 916.
[2] D. Bertsekas, Constrained Optimization and Lagrange Multiplier Methods, Computer Science and Applied Mathematics Series, Academic Press, San Diego, 1982.
[3] D. Bertsekas, Projected Newton methods for optimization problems with simple constraints, SIAM J. Control Optim. 20 (1982) 221.
[4] J.F. Bonnans, J.C. Gilbert, C. Lemarechal, C.A. Sagastizabal, Numerical Optimization—Theoretical and Practical Aspects, Springer, Berlin, 2002.
[5] A. Bressan, Hyperbolic Systems of Conservation Laws, Oxford University Press, Oxford, UK, 2000.
[6] R. Byrd, P. Lu, J. Nocedal, C. Zhu, A limited memory algorithm for bound constrained optimization, SIAM J. Sci. Comput. 16 (1995) 1190–1208.
[7] E.K.P. Chong, S.H. Zak, An Introduction to Optimization, Wiley-Interscience Series, 2000.
[8] G.M. Coclite, M. Garavello, B. Piccoli, Traffic flow on a road network, SIAM J. Math. Anal. 36 (6) (2005) 1862–1886.
[9] A.R. Conn, N.I.M. Gould, P.L. Toint, Trust-Region Methods, in: MPS/SIAM Series on Optimization, SIAM, Philadelphia, 2000.
[10] C.F. Daganzo, Requiem for second order fluid approximations of traffic flow, Transportation Res. Part B 29 (1995) 277.
[11] D. Helbing, Improved fluid dynamic model for vehicular traffic, Phys. Rev. E 51 (1995) 3164.
[12] D. Helbing, Verkehrsdynamik, Springer, Berlin, Heidelberg, New York, 1997.
[13] M. Herty, A. Klar, Simplified dynamics and optimization of large scale traffic networks, M^3AS 14 (4) (2004) 579–601.
[14] M. Herty, Mathematics of traffic flow networks, Ph.D. Thesis, TU Darmstadt, 2004.
[15] H. Holden, N. Risebro, A mathematical model of traffic flow on a network of unidirectional road, SIAM J. Math. Anal. 26 (4) (1995) 999–1017.
[16] R. Illner, A. Klar, M. Materne, Vlasov–Fokker–Planck models for multilane traffic flow, Comm. Math. Sci. 1 (2003) 1.
[17] C.T. Kelley, Iteravative Methods for Optimization, SIAM, Philadelphia, 1999.
[18] A. Klar, R. Wegener, Kinetic derivation of macroscopic anticipation models for vehicular traffic, SIAM J. Appl. Math. 60 (2000) 1749.
[19] R. Kühne, Macroscopic freeway model for dense traffic, in: N. Vollmuller (Ed.), Ninth International Symposium on Transportation and Traffic Theory, 1984, p. 21.
[20] J.P. Lebacque, Les modeles macroscopiques du traffic, Ann. Ponts. 67 (1993) 24–45.
[21] J. Lebacque, M. Khoshyaran, First order macroscopic traffic flow models for networks in the context of dynamic assignment, in: M. Patriksson, K.A.P.M. Labbe (Eds.), Transportation Planning-State of the Art, 2002.
[22] R.J. LeVeque, Numerical Methods for Conservation Laws, Birkhäuser-Verlag, Basel, 1990.
[23] M.J. Lighthill, G.B. Whitham, On kinematic waves: II. A theory of traffic flow on long crowded roads, Proc. Roy. Soc. London, Ser. A 229 (1955) 317–345.
[24] A. May, Traffic Flow Fundamentals, Prentice-Hall, Englewood Cliffs, NJ, 1990.
[25] H. Payne, FREFLO: a macroscopic simulation model for freeway traffic, Transportation Res. Record 722 (1979) 68.
[26] P. Spellucci, Numerische Verfahren der nichtlinearen Optimierung, Birkhäuser-Verlag, Basel, Boston, Berlin, 1993.
[27] C. Zhu, R. Byrd, J. Lu, J. Nocedal, L-BFGS-B: Fortran subroutines for large scale bound constrained optimization, Technical Report, NAM-11 EECS Department Northwestern University, 1994.